IEEE Access
Multidisciplinary | Rapid Review | Open Access Journal

Received September 5, 2019, accepted October 4, 2019, date of publication October 11, 2019, date of current version October 23, 2019.

Digital Object Identifier 10.1109/ACCESS.2019.2946710

Power Transfer and Multi-Control Mode of a Distribution Network Based on a Flexible Interconnected Device

TONGHUA WU[1,2,3], (Member, IEEE), YUPING ZHENG[1,2,3], (Senior Member, IEEE), HONGBIN WU[4], (Member, IEEE), HAO DONG[4], AND XIAOHONG WANG[2,3]

[1]College of Energy and Electrical Engineering, Hohai University, Nanjing 210098, China
[2]State Key Laboratory of Smart Grid Protection and Control, Nanjing 211106, China
[3]NARI Group Corporation, Nanjing 211106, China
[4]School of Electrical Engineering and Automation, Hefei University of Technology, Hefei 230009, China

Corresponding author: Tonghua Wu (wutonghua@sgepri.sgcc.com.cn)

This work was supported by Science and Technology Program of State Grid Corporation of China "Research on fault coupling characteristics and new protection principle of AC/DC hybrid power grid, 524608170147."

ABSTRACT With large-scale access to distributed power sources in medium and low-voltage distribution networks, the problem of insufficient local consumption capacity and source-charge mismatch in medium- and low-voltage distribution stations has become increasingly prominent. Power transfer and control strategies based on a flexible interconnection device (FID) for a distribution area near a particular geographical location are studied in this paper. A two-terminal distribution network model with tidal current complementarity is built based on a back-to-back (B2B) FID. A multi-mode operation method is proposed for power conversion under normal operation and power recovery under failure of one side, and a smooth switching strategy based on multiple control modes is also presented. Using this smooth switching method, an inverter controller is designed to form an integrated control unit. Finally, a simulation model of the distribution area with FID is built, and simulations of power transfer and mode switching under different working conditions are carried out. The correctness and effectiveness of the proposed method are verified.

INDEX TERMS Power transfer, flexible interconnection device, multi-control mode, power recovery, smooth switching strategy.

I. INTRODUCTION

As an important part of the power grid, the distribution network directly faces power users, and its mode of operation and any changes in state will affect the users' electricity consumption [1]-[3]. Following the rapid development of renewable energy sources and policy incentives for distributed power grids around the world, distributed power sources are not only connected to the grid through large-scale power stations; most have been directly connected to the grid via medium- and low-voltage distribution areas [4]-[7]. However, some medium- and low-voltage distribution stations have a large proportion of random loads, and large-scale distributed power grids cannot be absorbed, resulting in problems such as a time-space mismatch between the source and load [8]-[10]. Under these conditions, any power that cannot be absorbed will be sent to the high-level voltage network, which changes the power supply structure of the distribution network and also increases the loss, causing difficulties in the operation and maintenance of relay protection and measuring devices.

In medium- and low-voltage distribution areas, the local consumption of distributed power and the randomness of the load have received extensive attention in recent years [11]. The development and application of energy storage devices means that electrical energy that is not consumed in real time can now be stored [12], [13], although due to the investment costs and the energy storage capacity of some low-voltage power distribution stations, energy storage devices often cannot solve the fundamental problem of source-charge mismatch. The low-frequency load shedding method can solve the problem of source-charge mismatch to a certain extent [14], [15]; however, it is necessary to reduce the reliability of

The associate editor coordinating the review of this manuscript and approving it for publication was Shravana Musunuri.

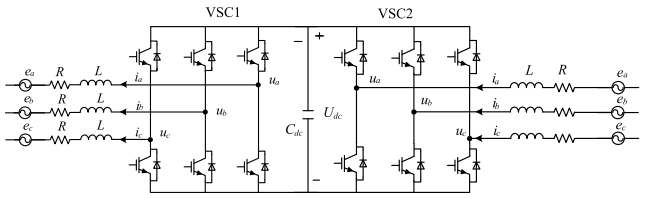

FIGURE 1. Basic structure of the B2B FID.

the power supply of the distribution network at the expense of some of the load power supply.

Studies in the literature [16], [17] have reported the benefits flow control, reactive power compensation and voltage regulation under normal network operating conditions, as well as fast fault isolation and supply restoration under abnormal conditions. A method has also been presented [18] to determine whether a FID is a viable alternative to other voltage control strategies for this particular application, and a case study considering the economic benefits of increasing feasible DG penetration was also carried out. A coordinated control method for an AC/DC hybrid distribution network with FID has been proposed [19], [20], although the mode of operation under failure is not considered in these papers.

This paper aims to address the problem of space-time mismatch between source and load in medium and low-voltage distribution areas. Under normal operating conditions, based on flexible DC interconnection technology, a double-terminal control strategy using a B2B FID is proposed that offers a power transfer method suitable for medium and low-voltage distribution areas. Considering the possible failures at the two terminals of the flexible DC interconnection device, and combined with the process when the two terminals are faulty, various control modes of the double-terminal inverter are available in order to achieve power transfer under normal operating conditions, and to mitigate the source-to-charge mismatch. A control strategy is proposed that includes a switching method for two interconnected converters when a fault occurs at either terminal. In the event of a fault, each terminal of the interconnection can supply power to the other terminal's load.

II. STRUCTURE AND FUNCTION OF A FLEXIBLE DC INTERCONNECTION DEVICE

A flexible DC interconnection device is generally implemented based on the full control device. The flexible operation control mode of the power electronic device can offer various functional architectures of the FID, including power transfer under normal operation conditions and fault recovery of the distribution network. For example, the topology of the B2B FID is as follows:

As shown in Fig.1, the FID is connected by a B2B converter through a DC capacitor. The two inverters are labeled as VSC1 and VSC2, respectively. Under normal and fault conditions, the two converters will adopt different control modes and complete control strategy-switching at the moment of failure.

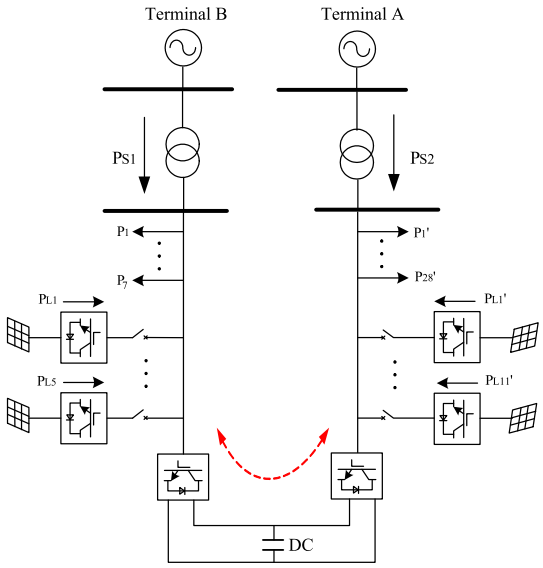

FIGURE 2. Flexible interconnection structure in a low-voltage distribution network.

The structure which connected in medium and low-voltage distribution networks is shown in Fig.2 below.

As shown in Fig.2, two low-voltage power distribution stations are connected by a B2B FID. The FID contains a bidirectional power converter, and both terminals A and B can realize bidirectional transfer of the power flow through the FID. The two inverters are controlled by a central controller of active and reactive power; this is not only needed to stabilize the DC voltage, but can also allow system operation under normal and partial fault conditions. In a particular area, the distributed power generation permeability may be higher, resulting in excess power, while other areas may have a higher load density. Power can be transferred to the two stations through the FID connection, improving the capacity of the distributed power output and alleviating the power shortage at the station. When a fault occurs in one terminal zone, the other terminal can supply several important loads within the faulty area, thus improving the reliability of the power supply in the low-voltage area of the distribution network.

III. FID-BASED MULTI-MODE CONTROL MODEL FOR DISTRIBUTION STATION AREA

A. FID-BASED DISTRIBUTION AREA FAILURE RECOVERY METHOD

Due to the access of the FID, a two-way power supply can be realized at both terminals A and B under normal operating conditions, while in the case of a fault, the FID can assist in recovery of the power supply of the faulty terminal. However, as a power electronic device involved in fault recovery, FID cannot supply power to all de-energized areas in the event of a fault. The recovery process after a failure is as follows: when a fault occurs at one terminal, the FID is first locked, and the line relay protection device of the fault is also engaged. After the fault is removed, the FID is used to provide power to the faulty part of the load from the non-faulty terminal.

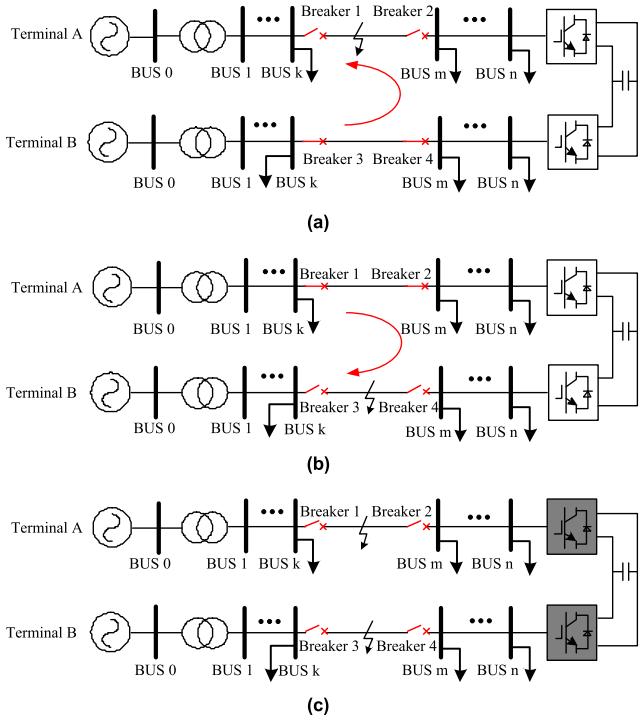

FIGURE 3. Power supply mode for the FID distribution network under different fault conditions(a) The A terminal is shorted and cut off, and the B terminal supplies power to it. (b) The B terminal is short-circuited and cut off, and the A terminal supplies power to it. (c) Double-terminal short circuit and cut off: inverter blocking.

Based on this, after the action of the relay protection device in different situations is established, the fault recovery method of the distribution network area with FID is shown in Fig.3.

When the distribution network fails, the positioning and isolation of the relay protection device causes a certain area of power loss to be formed. As shown in Fig.3, based on the relative position of the fault point and the FID mounting point, the following three fault recovery methods are applicable:

a. When terminal A fails and is cut off, circuit breakers 1 and 2 are opened. Terminal A loses power, and terminal B supplies power to the partial load on terminal A through the FID.

b. When terminal B fails and is cut off, circuit breakers 3 and 4 are opened. Terminal B loses power, and terminal B supplies power to the partial load on terminal B through the FID.

c. When both terminals A and B fail and are cut off, circuit breakers 1, 2, 3 and 4 are opened, and both terminals lose power. At this point, the double-terminal FID is blocked.

B. MULTI-MODE MODEL WITH FID IN RADIO AREA

In normal operation and when different types of faults arise as described in the previous section, the two inverters will operate with different control strategies. Under normal circumstances, the control target is the transfer of power; that is, the transfer is performed according power setting within a certain range. When one terminal fails and loses power, the voltage at the fault terminal needs to be stabilized

TABLE 1. FID control mode under different operating conditions.

Control mode	VSC1	VSC2
A	PQ	P-V_{dc}
B	VF	P-V_{dc}
C	P-V_{dc}	VF

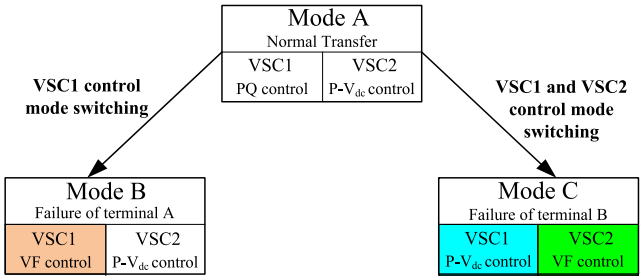

FIGURE 4. Multi-state model based on the FID distribution network.

while maintaining a partial load power supply. Various control methods for the FID are therefore proposed, as shown in Table 1.

It can be seen from Table 1 that the double-terminal converters of the FID apply different control strategies under different operating conditions. Hence, a multi-state model based on the FID distribution network can be proposed, as shown in Fig.4 below.

As shown in Fig.4, under normal circumstances, the double-terminal converter works in the normal transfer mode, labeled as mode A. If a fault occurs at terminal A, then in order to maintain the power failure terminal voltage and achieve fault recovery, VSC1 switches from PQ control to VF control, which is labeled as mode B. In the case where terminal B fails and is cut off, if the control strategy of VSC2 is switched to VF control only by referring to mode B, the B2B converter will form PQ+VF control. At this time, the intermediate capacitor link loses the voltage regulation mechanism, which will cause a large drop in the DC voltage, and cause the power failure to recover from the power loss terminal. Therefore, the control strategy of VSC1 is also switched to P-$V_{\rm dc}$ control. The control status at this time is recorded as mode C. The FID-based distribution network multi-state model is thus formed. When the inverter performs control strategy switching, if multiple sets of control devices are used, it is easy to cause hard switching, resulting in system instability. In the next section, we examine smooth switching in each mode.

IV. FID-BASED MULTI-MODE SMOOTH SWITCHING STRATEGY

A. SMOOTH SWITCHING STRATEGY FROM MODE A TO MODE B

It is easy to see that the switch between mode A and mode C involves the VSC1 controller switching from PQ control to VF control. The basic structure of PQ control is shown below:

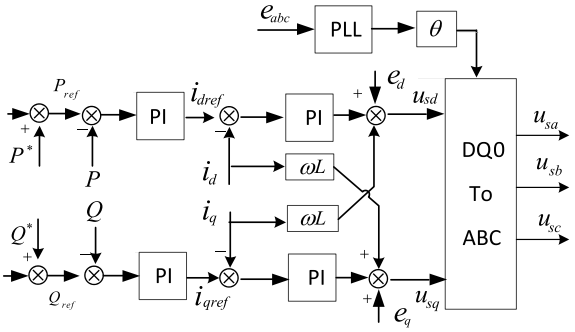

FIGURE 5. Block diagram for PQ control structure.

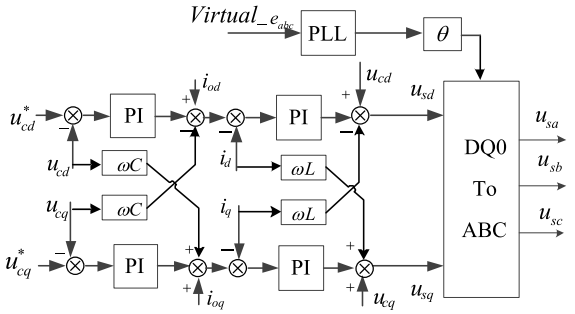

FIGURE 6. Block diagram for VF control.

In Fig.5, the difference between the active power and the reactive power is adjusted by the PI to obtain the reference values i_{dref}, i_{qref} of the inner loop inductor current i_{d}, i_{q}. The inductor current reference values i_{dref} and i_{qref} are compared with their measured value through the PI regulator to get the modulation wave voltage, which is used to control the SPWM.

The purpose of the constant voltage and frequency control (VF control) is to ensure that the voltage amplitude and frequency of the common AC bus connected to the inverter power supply are unchanged when the output of the power supply changes. The theoretical derivation process of the VF controller structure is similar to the derivation process of the PQ controller; the same current inner loop control mode but different outer loop control modes are used. The control structure is as shown in Fig.6 below.

The reference value of the current inner loop is obtained after the reference value and the measured value of the capacitor voltage pass through the PI regulator. The reference value and its measured value then pass through the PI regulator to give a modulated wave voltage for controlling the SPWM.

It can be observed from the above analysis that there are two main differences between PQ control and VF control: (i) the current inner loop command value is given differently, in that PQ control is a power loop, while VF control is a voltage loop; and (ii) the phase angles are obtained differently. In PQ control mode, the phase angle is obtained based on information about the grid side voltage, while in VF control mode, due to the grid fault and other reasons, the reference

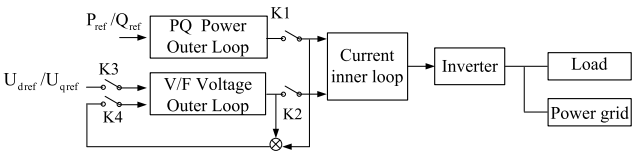

FIGURE 7. Smooth switching control from PQ to VF control.

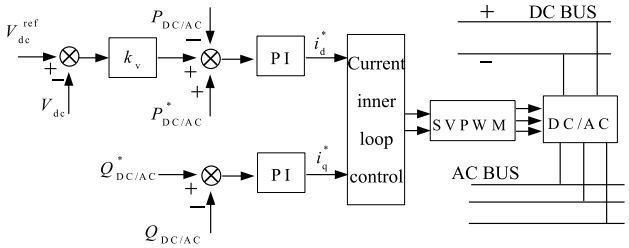

FIGURE 8. Block diagram of power-voltage sag control.

of the voltage and frequency of the grid is lost, and the phase angle needs to be calculated internally.

According to this, in order to reduce the adverse effects incurred to the system by the control strategy switching, this paper proposes a smooth switching control method based on controller state following. The specific method is illustrated in Fig.7 below.

The VF controller state and the output of the PQ controller are designed to give negative feedback to the input of the VF controller, so that the VF controller can follow the output of the PQ controller at any time before switching; this ensures that the output states of the two controllers are consistent at all times. At the same time, the logic switches K1∼K4 are controlled reasonably: during normal operation, switches K1 and K4 are closed, and switches K2 and K3 are open, and when switching, switches K1 and K4 are open and switches K2 and K3 are closed. In order to ensure smoothing of the switching process, the transient oscillation in the system caused by the phase angle of the voltage, given by the switching instant system and the phase angle at the previous moment of switching, is prevented. The phase angle θ should be given at the time of switching, before the switching phase. The angle is integrated based on the angle of the voltage phase at the moment before switching, as follows:

$$\theta = \theta_{\mathrm{grid}} + \frac{\omega_{\mathrm{ref}}}{s} \tag{1}$$

B. SMOOTH SWITCHING STRATEGY FROM MODE A TO MODE C

When mode A switches to mode C, VSC2 needs to switch to VF control, and VSC1 also switches from PQ control to P-V_{dc} control to stabilize the DC capacitor voltage. In this paper, the VSC2 is applied with power-voltage (P-V_{dc}) droop control under normal operating conditions, and the DC bus voltage pair can be adjusted according to the power supply. The control structure is shown in Fig.8 below.

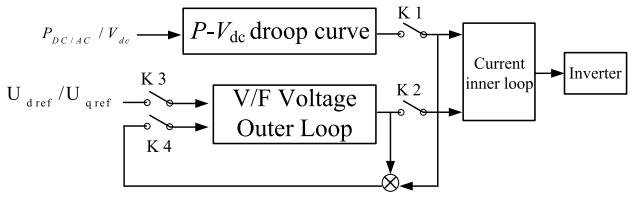

FIGURE 9. Smooth switching between P-V_{dc} control and VF control.

It is easy to see that the current inner loop structure of the P-V_{dc} control is the same as both the PQ control and the VF control, and it is therefore designed as a common current inner loop control when the control strategy is switched. When mode A is switched to mode C, VSC2 needs to be switched from P-V_{dc} to VF. The smooth switching principle is similar to the state following system of PQ and VF. The structure diagram is shown in Fig.9.

The switching operation sequence of the switching strategy is the same as that in Fig.8, and in order to prevent the system from oscillating during switching, the integral link in (1) is also matched.

It can be seen from the above control structure that the two control strategies have many similarities, so the VSC1 stabilized DC voltage link is used for P-V_{dc} control. The only difference between PQ control and P-V_{dc} control is that in the latter, the q-axis command value iq of the current inner loop is given differently, and the d-axis current command value is the same. Moreover, the phase angle acquisition methods of the two control modes are the same, and there is thus no need to perform phase angle smooth switching.

C. INTEGRATED CONTROL SYSTEM FOR VSC1 AND VSC2

Combining the above several control mode switching modes, it is easy to see that at device level, VSC1 needs to have two functions of smooth switching from PQ control, i.e. not only to VF control but also to P-V_{dc} control, and VSC2 needs to have the function of smooth switching from P-V_{dc} control to PQ control. This imposes higher requirements for the control system of the inverter. Based on the principle of the same current inner loop, the proposed system minimizes the workload and impact of the control mode switching. Integrated control methods are proposed as shown in Fig.10.

As shown in Fig.10, both VSC1 and VSC2 are based on a common current inner loop control strategy that minimizes the amount of work required for switching. VSC2 is applied to the smooth switching strategy of PQ and VF control. The switching strategy based on Fig.7 and by (1) is illustrated in Fig.11.

In PQ control mode, switches S1 and S2 are closed at position 1, and the phase of the control system is the phase of the grid-connected voltage of the converter. In VF control mode, S1 and S2 are turned off at position 2, and the recording section records the voltage phase angle before PQ control is switched to VF control.

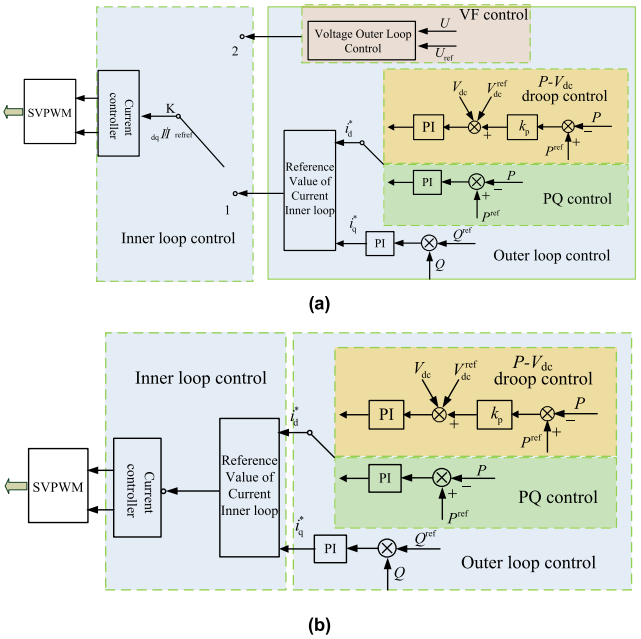

FIGURE 10. Bidirectional inverter integrated control. (a) VSC1 control mode. (b) VSC2 control mode.

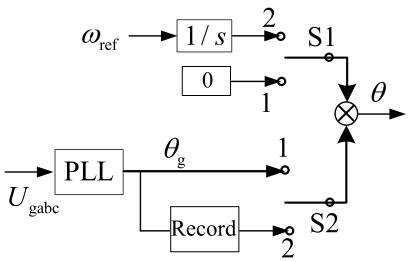

FIGURE 11. Smoothing switching control for phase angle.

V. CASE ANALYSIS

In order to analyze and verify the control method proposed in this paper, the study model shown in Fig.2 was built. The terminal voltage of the A and B was 10kV, and the voltage was reduced by a 10kV/380V transformer. The terminals of the two zones were connected by a FID. To ensure that when a fault occurs on one side of the FID, the other side can supply power to the important load on the side, and to avoid power redundancy [21], the rated power of the FID is set to 84 kW according to the load condition at both ends.

In order to study the operation of the system under different conditions, an analysis was carried out of the following three cases.

A. POWER TRANSFER SIMULATION IN NORMAL OPERATION MODE

As shown in Fig.12, Take the loads at both terminals of A and B as shown in Table 2.

At this time, the system is operated in mode A, VSC1 is in PQ control, and VSC2 is in P-V_{dc} control. In the initial state,

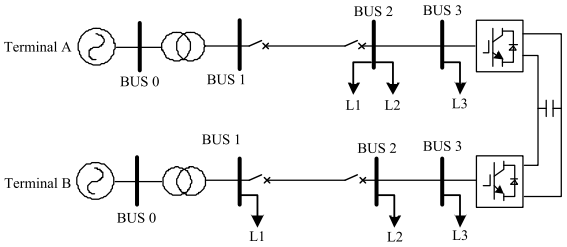

FIGURE 12. Structure of the example system.

TABLE 2. Load value.

	Terminal A	Terminal B
L1	45 kW, 20 kVar	45 kW, 20 kVar
L2	25 kW, 6 kVar	35 kW, 6 kVar
L3	20 kW	20 kW

TABLE 3. Details of case and timing.

Time	0-5s	5-7s	7-10s	10-15s
Light intensity (W/m^2)	600	1000	1000	1000
Transfer power (kW)	20 (A→B)	30 (A→B)	10 (A→B)	20 (B→A)
Loads on terminal A	L1 L2	L1 L2	L1 L2	L1 L2 L3
Loads on terminal B	L1 L2 L3	L1 L2 L3	L1 L2	L1 L2

three loads are connected at terminal B, and only LOAD1 and LOAD2 are connected at terminal A. At time 0–5 s, the light intensity of the terminal A photovoltaic power generation system is 600 W/m^2. Due to insufficient capacity for consumption at terminal A, the power transferred to terminal B is set at 20 kW. At time 5–7 s, the light intensity is enhanced to 1000 W/m^2, and the consumption capacity is lower. Considering the load demand at terminal B, the power transfer is set to 30 kW. At time 7 s, LOAD3 at terminal B is cut off, meaning that the power demand at terminal B is reduced, and the transfer power is set to 10 kW. At time 10 s, LOAD3 is input to terminal A. At this time, the power transfer is reversed, and the power from terminal B to terminal A is 20 kW. Details are shown in Table 3.

The simulation results are shown below.

Fig.13 shows the simulation results in mode A, that is, in a normal transfer situation. As shown in Fig.13(a), after 5 s, the illumination is enhanced, and the photovoltaic output is increased by about 20 kW. As shown in Fig.13(b), when the direction of power transfer changes at 10 s, the AC voltage at terminal direction does not fluctuate significantly, but maintains a stable level. Fig.13(c) shows the active power flowing through the transformers at both terminals. It can be seen that the magnitude of the transfer power directly affects the current flow of each terminal line and changes the local consumption rate. Finally, it can be seen from Fig.13(d) that the value set for active power transfer in the set working condition

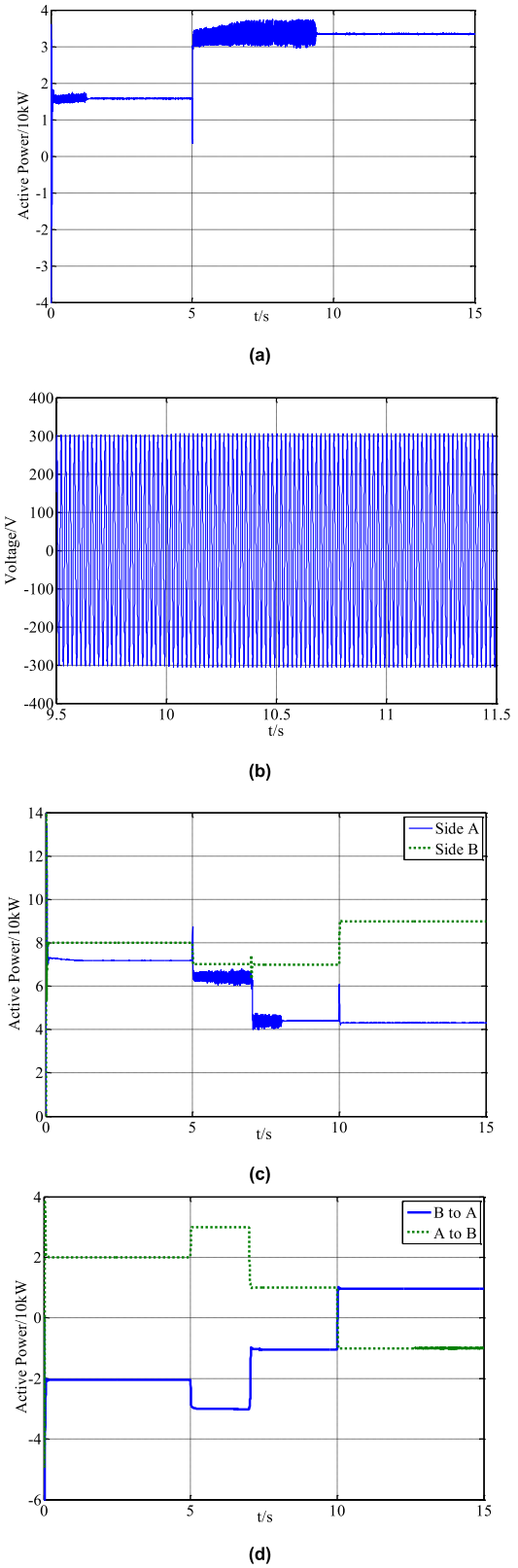

FIGURE 13. Simulation results in mode A. (a) Output power of the photovoltaic system. (b) AC voltage at terminal A. (c) Power flowing through the transformer. (d) Power transfer through FID.

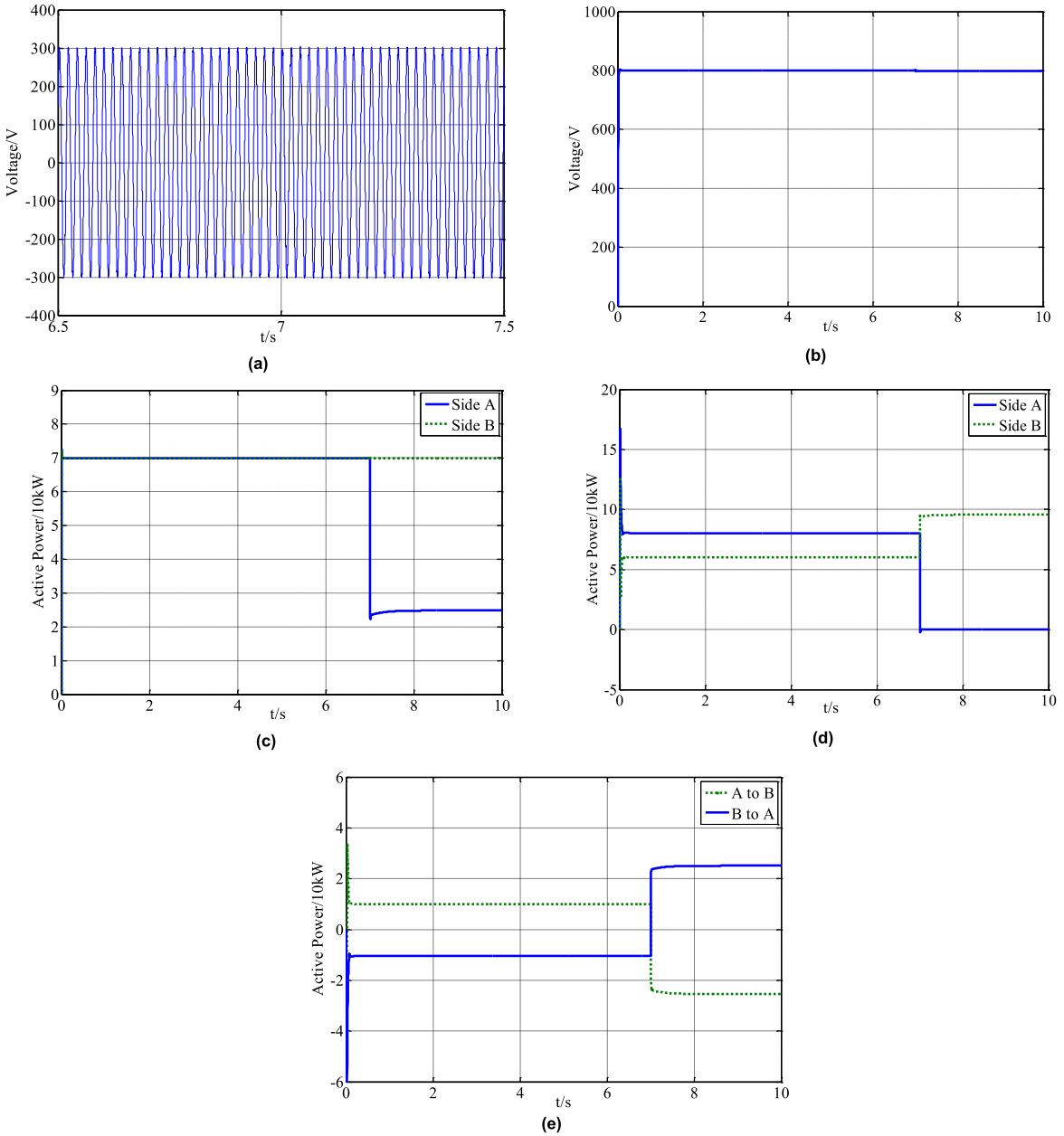

FIGURE 14. Simulation results in mode B. (a) AC voltage at terminal A. (b) DC capacitor voltage. (c) Load level at both terminals. (d) Power flowing through the transformer. (e) Transfer power through the FID.

is verified in the simulation. At time 0–5 s, the power from terminal A to terminal B is 20 kW. At time 5–7 s, the power transfer is 30 kW. At time 7–10 s, the power transfer is 10 kW. After 10 s, the direction of power transfer is reversed, and it becomes 20 kW from terminal B to terminal A.

Under different conditions, after the system reaches a steady state, the power loss of the FID calculated by (2) is shown in Table 4.

$$P_{\text{loss}} = P_{\text{in}} - P_{\text{out}} \tag{2}$$

where, P_{loss} is the power loss of FID, P_{in} is the input power of FID, and P_{out} is the output power of FID.

TABLE 4. Power loss of FID.

Time	0-5s	5-7s	7-10s	10-15s
Input power (kW)	20.4	30.3	10.4	-9.57
Output power (kW)	20.0	30.0	10.0	-10
Power loss (kW)	0.4	0.3	0.4	0.43
System efficiency	98.0%	99.0%	96.2%	95.7%

It can be seen that the higher the transfer power of FID is, the higher the transfer efficiency is. The efficiency of FID can be maintained at more than 95% with different transfer

TABLE 5. Changes of loads and operation mode.

Time	0-7s	7-10s
Loads on terminal A	L1 L2	L2
Loads on terminal B	L1 L2	L1 L2
Mode of operation	mode A	mode B

power. The effectiveness of this control method in the steady state operation of the system is verified.

B. FAULT RECOVERY SIMULATION UNDER A-SIDE FAULT CONDITION

There are only two loads at terminal A: L1 (45 kW, 20 kVar) and L2 (25 kW, 6 kVar). There are also only two loads at terminal B: L1 (45 kW, 20 kVar) and L2 (25 kW, 6 kVar). In the initial state, both loads are connected. At this time, the system is operating in mode A, VSC1 is in PQ control, and VSC2 is in P-V_{dc} control. At time 7 s, the short circuit fault occurs between BUS1 and BUS2, the protection moves quickly and the faulty line is cut off, and the photovoltaic is off-grid, which causes the downstream line and load of BUS2 to lose power. At this time, the mode of operation of the system is switched to mode B, according to the seamless switching policy described in Section 3. Due to the limited power provided by terminal B, part of the minor load LOAD1 is removed at terminal A, and the main load LOAD2 is retained. Details are shown in Table 5.

The simulation results are shown below.

The simulation results are shown in Fig.14 for mode B, that is, the fault at terminal A. As shown in Fig.14(a), under the A-side fault condition, VSC1 is switched to the A-side BUS3 AC voltage after VF control. It can be seen that the AC voltage maintains a normal voltage level without a significant drop. The DC capacitor voltage level is shown in Fig.14(b). It can be seen that when the fault occurs, VSC2 is switched to P-V_{dc} control to effectively stabilize the DC voltage without significant oscillation. Load levels at both terminals are shown in Fig.14(c), and the active power flowing through the transformer is shown in Fig.14(d). As can be seen from Fig.14(e), when terminal A fails, the active power is supplied in reverse according to the setting, which ensures power supply to the important load at terminal A. It can be seen from the above simulation results that at 7 s, the AC and DC voltages are stable and the power is transferred according to the instructions.

C. FAULT RECOVERY SIMULATION UNDER B-SIDE FAULT CONDITION

As shown in Fig.12, the three loads at the A terminal are: L1 (45 kW, 20 kVar); L2 (25 kW, 6 kVar); L3 (30 kW). The loads at the B side are: L1 (45 kW, 20 kVar) and L2 (25 kW, 6 kVar). At 3 s, the L3 at terminal A is cut off. At this time, the capacity for consumption at terminal A is insufficient, and the active power is 30 kW to terminal B. At time 7 s, a short circuit fault occurs at terminal B, the secondary load L1 is removed,

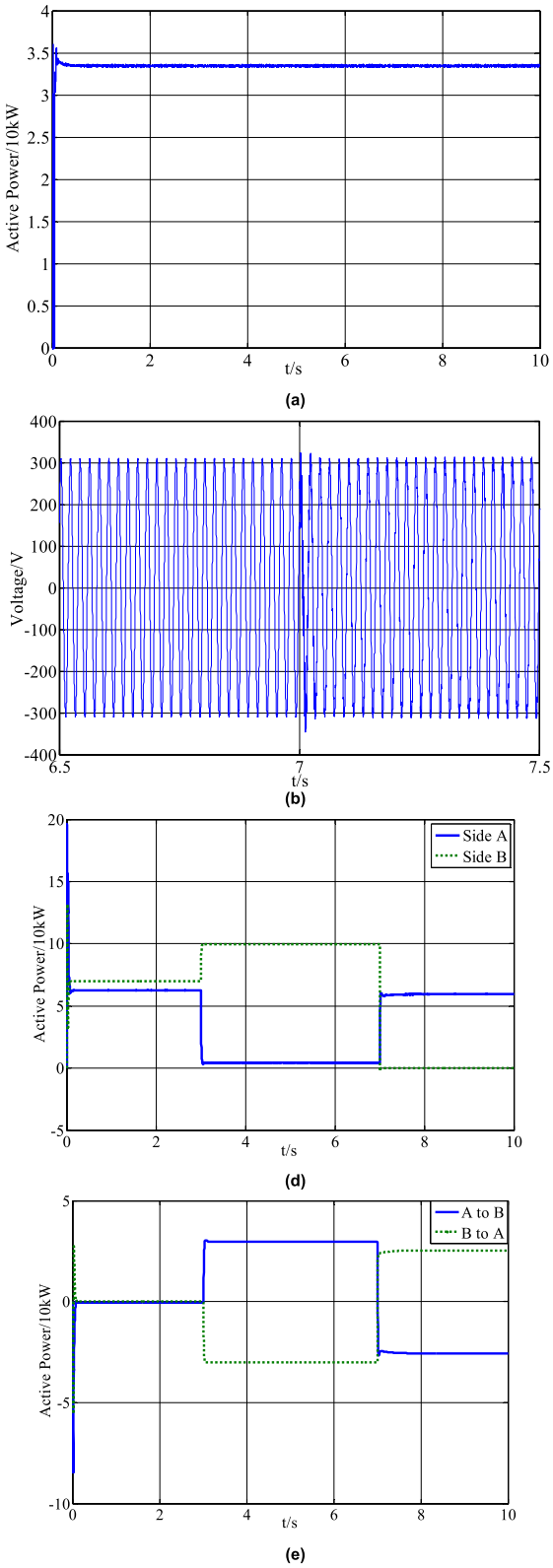

FIGURE 15. Simulation results in mode C. (a) Output power of the photovoltaic system. (b) AC voltage at terminal A. (c) DC capacitor voltage. (d) Power flowing through the transformer. (e) Transfer power through the FID.

TABLE 6. Changes of loads and operation mode.

Time	0-3s	3-7s	7-10s
Loads on terminal A	L1 L2 L3	L1 L2	L1 L2
Loads on terminal B	L1 L2	L1 L2	L2
Mode of operation	mode A	mode A	mode C

the main load L2 is retained, and terminal A supplies power to terminal A through the FID. To maintain the B-side AC voltage, the smoothing strategy described in Section 2 is used to switch VSC2 to VF control, that is, switching from mode A to mode C. Details are shown in Table 6.

The simulation results are shown below.

Fig.15 shows the simulation results in mode C, i.e. a fault at terminal B. The output power of the photovoltaic system is shown in Fig.15(a). As shown in Fig.15(b), under the B-side fault condition, VSC2 is switched to the B-side BUS3 AC voltage after VF control. It can be seen that the AC voltage maintains a normal voltage level without a significant drop. The DC capacitor voltage level is shown in Fig.15(c). It can be seen that when the fault occurs, the P-V_{dc} control of VSC1 effectively stabilizes the DC voltage without obvious oscillation. The active power flowing through the transformer is shown in Fig.15(d). It can be observed that the active power flowing through the transformer after the failure at time 7 s is zero. Fig.15(e) shows that at time 3–7 s, the system transfers 30 kW from terminal A to terminal B, according to the set value. In the case of failure at terminal B, the active power is supplied in reverse according to the set value, which ensures the supply of the important loads at terminal A.

In summary, in mode A, that is, in normal operation, the FID-based system performs accurately according to the command value. When a fault occurs at terminal A, the mode is smoothly switched from mode A to mode B. The AC and DC voltages at terminal A show no obvious oscillation, and terminal B can supply the important load at terminal A. When the fault occurs at terminal B and the faulty line is cut off, the mode of operation of the system is smoothly switched from mode A to mode C. The AC and DC voltages at terminal B have no obvious oscillation, and terminal A can supply the important load at terminal B, which verifies the correctness and effectiveness of the proposed switching strategy

VI. CONCLUSION

In this paper, power transfer and fault recovery of a distribution network based on a B2B FID are studied. A FID-based multi-mode control method for distribution station interval is proposed, and seamless switching strategies between different modes are studied. The main conclusions are as follows:

1) In the distribution network, effective power transfer between multiple stations can be achieved through a FID, which can improve the low consumption capacity of high-permeability distributed generation areas, prevent power from being transferred back to the main power grid and improve the reliability of the power supply.

2) Multi-mode control based on a FID can ensure that each of the two stations connected by the FID can be supplied with power through the other terminal if one fails. After the protective action, the important load in the power-loss area can be supplied to improve the self-healing ability of the distribution network.

3) The multi-mode seamless switching strategy proposed in this paper ensures seamless switching of the control modes of the two VSCs in the FID at the time of failure, and does not introduce severe oscillation or instability factors to the system. It provides a theoretical basis for the participation of a FID in power transfer and fault recovery under different conditions.

REFERENCES

[1] A. Yazdani and P. P. Dash, "A control methodology and characterization of dynamics for a photovoltaic (PV) system interfaced with a distribution network," *IEEE Trans. Power Del.*, vol. 24, no. 3, pp. 1538–1551, Jul. 2009.
[2] D. Ambrosino, "Distribution network design: New problems and related models," *Eur. J. Oper. Res.*, vol. 165, no. 3, pp. 610–624, 2005.
[3] Y. You, D. Liu, and Y. U. Wenpeng, "Technology and its trends of active distribution network," (in Chinese), *Automat. Electr. Power Syst.*, vol. 36, no. 18, pp. 10–16, 2012.
[4] N. Acharya, P. Mahat, and N. Mithulananthan, "An analytical approach for DG allocation in primary distribution network," *Int. J. Elect. Power Energy Syst.*, vol. 28, no. 10, pp. 669–678, Dec. 2006.
[5] S. A. Papathanassiou, "A technical evaluation framework for the connection of DG to the distribution network," *Electr. Power Syst. Res.*, vol. 77, no. 1, pp. 24–34, 2007.
[6] C. Wei, Y. Fu, and Z. Li, "Optimal DG penetration rate planning based on S-OPF in active distribution network," *Neurocomputing*, vol. 174, pp. 514–521, Jan. 2016.
[7] R. Arulraj and N. Kumarappan, "Optimal single and multiple DG installations in radial distribution network using SLPSO algorithm," *Intell. Efficient Elect. Syst.*, vol. 446, pp. 89–96, Dec. 2018.
[8] Z. Wu, H. Tazvinga, and X. Xia, "Demand side management of photovoltaic-battery hybrid system," *Appl. Energy*, vol. 148, pp. 294–304, Jun. 2015.
[9] Y. Ren, P. N. Suganthan, N. Srikanth, and G. Amaratunga, "Random vector functional link network for short-term electricity load demand forecasting," *Inf. Sci.*, vols. 367–368, pp. 1078–1093, Nov. 2016.
[10] H. Wu, P. Dong, and M. Liu, "Random fuzzy power flow of distribution network with uncertain wind turbine, PV generation, and load based on random fuzzy theory," *IET Renew. Power Gener.*, vol. 12, no. 10, pp. 1180–1188, 2018.
[11] L. F. Ochoa, C. J. Dent, and G. P. Harrison, "Distribution network capacity assessment: Variable DG and active networks," *IEEE Trans. Power Syst.*, vol. 25, no. 1, pp. 87–95, Feb. 2010.
[12] S. Xinwei, Z. Shouzhen, and Z. Jinghong, "Active distribution network planning-operation co-optimization considering the coordination of ESS and DG," (in Chinese), *Power Syst. Technol.*, vol. 39, no. 7, pp. 1913–1920, 2015.
[13] B. Dunn, H. Kamath, and J.-M. Tarascon, "Electrical energy storage for the grid: A battery of choices," *Science*, vol. 334, no. 6058, pp. 928–935, 2011.
[14] W. P. Luan, M. R. Irving, and J. S. Daniel, "Genetic algorithm for supply restoration and optimal load shedding in power system distribution networks," in *Proc. IEE Gener. Transmiss. Distrib.*, 2002, pp. 145–151.
[15] J. A. Short, D. G. Infield, and L. L. Freris, "Stabilization of grid frequency through dynamic demand control," *IEEE Trans. Power Syst.*, vol. 22, no. 3, pp. 1284–1293, Aug. 2007.
[16] W. Cao, J. Wu, N. Jenkins, C. Wang, and T. Green, "Benefits analysis of Soft Open Points for electrical distribution network operation," *Appl. Energy*, vol. 165, pp. 36–47, Mar. 2016.
[17] M. Masuda, E. Bormio, and J. A. Jardini, "Development and implementation of FACTS (flexible AC transmission systems) devices in distribution networks," in *Proc. IEEE/PES Transmision Distrib. Conf. Expo.*, Sao Paulo, Brazil, Nov. 2004, pp. 137–142.

[18] J. M. Bloemink and T. C. Green, "Increasing distributed generation penetration using soft normally-open points," in *Proc. IEEE PES Gen. Meeting*, Providence, RI, USA, Jul. 2010, pp. 1–8.
[19] Z. Xue, P. Wei, and F. Shixiong, "Coordinated control method of AC/DC hybrid distribution network with multi-terminal flexible interconnection devices," (in Chinese), *Automat. Electr. Power Syst.*, vol. 42, no. 7, pp. 185–191, Apr. 2018.
[20] P. Wang, C. Jin, D. Zhu, Y. Tang, P. C. Loh, and F. H. Choo, "Distributed control for autonomous operation of a three-port AC/DC/DS hybrid microgrid," *IEEE Trans. Ind. Electron.*, vol. 62, no. 2, pp. 1279–1290, Feb. 2015.
[21] X. Jun, J. Xun, and H. Renle, "Capacity dimensioning method of partitioned flexible interconnection device in urban power network," (in Chinese), *Automat. Electr. Power Syst.*, vol. 42, no. 2, pp. 99–105, 2018.

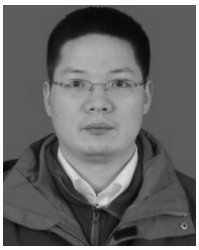

TONGHUA WU received the master's degree from the State Grid Electric Power Research Institute, Nanjing, China, in 2005. He is currently pursuing the Ph.D. degree in automation of electric power systems with Hohai University. His research interest includes relay protection and control of AC/DC hybrid power systems.

YUPING ZHENG received the B.Sc. degree from the Hefei University of Technology, Hefei, Anhui, in 1983, the M.Sc. degree from the Nanjing Automation Research Institute, in 1986, and the Ph.D. degree from Wuhan University, Wuhan, Hubei, in 2004. His research interest includes relay protection and control of AC/DC hybrid power systems.

HONGBIN WU received the B.Sc., M.Sc., and Ph.D. degrees in electrical engineering from the Hefei University of Technology, Hefei, China, in 1994, 1998, and 2005, respectively, where he is currently a Professor. His research fields include distributed generation technology, and distribution network modeling and simulation.

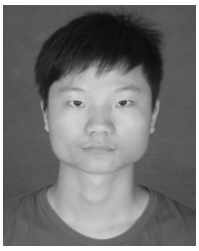

HAO DONG received the B.S. degrees in electrical engineering and automation from the Hefei University of Technology, in 2016, where he is currently pursuing the M.S. degrees in power system and automation. His research interest includes distributed power generation technology.

XIAOHONG WANG received the master's degree from the State Grid Electric Power Research Institute, Nanjing, China, in 1996. Her interests include AC/DC converter, SVC/SVG, and their applications in AC/DC hybrid power systems.